Materials & Design 212 (2021) 110252

Contents lists available at ScienceDirect

Materials & Design

journal homepage: www.elsevier.com/locate/matdes

Tunable photo-patterning of organic color-centers

Qingqing Dou [a], Beibei Xu [a,*], Xiaojian Wu [b], Junyao Mo [a], YuHuang Wang [b,c,*]

[a] State Key Laboratory of Modern Optical Instrumentation, School of Optical Science and Engineering, Zhejiang University, Hangzhou, Zhejiang 310027, China
[b] Department of Chemistry and Biochemistry, University of Maryland, College Park, MD 20742, United States
[c] Maryland NanoCenter, University of Maryland, College Park, MD 20742, United States

HIGHLIGHTS

- Photo-patterning strategy is developed to realize scalable localization of color-centers with high spatial accuracy.
- Light-stimulation can promote the functionalization of SWCNTs films forming organic color-centers.
- The patterns can be modulated by varying the chemical properties of the solvents.

GRAPHICAL ABSTRACT

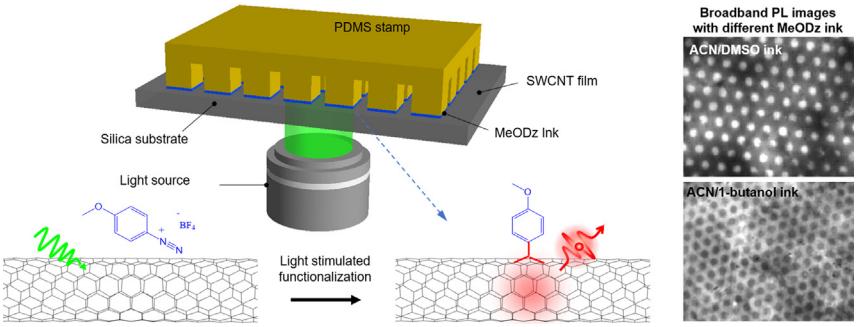

ARTICLE INFO

Article history:
Received 19 August 2021
Revised 13 November 2021
Accepted 14 November 2021
Available online 16 November 2021

Keywords:
Organic color-center
Photo-patterning
Spatial accurate localization
Optoelectronics

ABSTRACT

Organic color-centers (OCCs) in single-walled carbon nanotubes (SWCNTs) have been intensively investigated for quantum technologies, bio- and chemical sensing, bioimaging. The precise localization of OCCs at a scalable manner will bring about a revolution into next generation optoelectronics, which, however, remains a great challenge till now. Here, a scalable, low cost and universal photo-patterning strategy is developed to implant OCCs at desired locations on (6,5)-chirality SWCNT films by combining optically active diazonium chemistry and micro-contact printing methods. Notably, the patterns can be tunable by changing the solvents used for the patterning chemistry, affording control over the weight of diazonium salts at different regions. A systematic investigation reveals that the solvent properties (polarity and vapor pressure), the volume and concentration of ink used, the patterning methods, and the concentration of MeODz all contribute to the tunable patterning. This spatial accurate and solvent tunable photo-patterning technique is simple, scalable, and amenable to the integration of other color center chemistries and 2D transition metal dichalcogenides for the next-generation chip-integrated nanoelectronics and optoelectronics with high device uniformity and manipulability at molecular level.

1. Introduction

OCCs in SWCNTs are sp^3 quantum defects produced by covalent bonding of organic molecules to sp^2 carbon lattice of SWCNTs.[1] These point defects provide chemically tailored exciton traps where electrons, excitons, phonons and spin can couple to alter the collective physical and chemical properties of the host crystals and impart new quantum properties [1]. The unique properties introduced by OCCs have enabled the exploration of a whole array of potential novel applications, including quantum technologies [2,3], bio- and chemical sensing [4,5], and bioimaging [6]. For example, OCCs can emit single photon at room temperature with tunable emission wavelength covering the entire optical communication windows, demonstrating the potential for quantum communications [7]. However, current chemistries do not provide

* Corresponding authors.
E-mail addresses: bbxu2019@zju.edu.cn (B. Xu), yhw@umd.edu (Y. Wang).

https://doi.org/10.1016/j.matdes.2021.110252
0264-1275/

control over the spatial distribution of OCCs, which would be required for the development of next generation chip-integrated optoelectronic devices based on OCCs [1,8,9]. This problem can be addressed to some extent by applying printing techniques such as micro-contact printing, which is a low cost, versatile method compatible with integrated optoelectronic devices [10], surface chemistry [11], and biomedicine [12], to deliver molecular OCC precursors only at defined locations. In this context, an in-depth investigation of the printing chemistry is imperative to achieving high spatial resolution patterning of OCCs for the micro- and nano-integration.

Here, we demonstrated the feasibility of this solution using micro-contact printing to print 4-Methoxybenzenediazonium tetrafluoroborate (MeODz) on top of (6,5)-SWCNTs films. Light-stimulation then promotes the reaction of MeODz with SWCNT films to form patterned OCCs. By varying the chemical polarity and vapor pressure of the solvents, enabling the precise and scalable control of the weight of MeODz salts at different positions, the shape of OCCs patterns can be tunable with just one-single type of PDMS stamp.

2. Material and methods

2.1. Preparation of high purity (6,5)-SWCNT thin-films

High purity (6,5)-SWCNTs solution was prepared according to our previous methods using CoMoCAT SG65i SWCNTs (lot no. SG65i-L39) as raw materials [13]. It was then diluted to 3.18 μg mL^{-1} with sodium deoxycholate (DOC, 0.025% w v^{-1} Sigma Aldrich, >97%) in aqueous solution. SWCNT films were prepared by vacuum filtration with all the tubes aligned by carefully control the filtration speed using the procedure reported previously [14]. Nuclepore track-etched polycarbonate hydrophilic filter membranes with a diameter of 2.5 cm and pore size of 80 nm was used. 1 mL diluted SWCNT solution was filtered to obtain ultra-thin layers of film. The volume and concentration of SWCNT solution was carefully controlled to get the desired thickness of films [14]. The films were transferred onto silica substrate with the film-side down using a wet-transfer method [15]. The membrane was dissolved away by chloroform and then washed by acetone and deionized water. The thin-films were then annealed in vacuum at 300 °C for 8 min and 400 °C for 5 min to remove the majority of the surfactant molecules.

2.2. Photo-patterning of OCCs on CNT thin-films

PDMS stamp was prepared using standard photolithography methods [10]. Solvent ink containing different concentrations of MeODz in Acetonitrile (ACN)/Dimethyl sulfoxide (DMSO) (v:v = 1:3), ACN/1-butanol (v:v = 1:3) or water was coated onto the surface of PDMS stamps by cotton swabs. ACN is a good solvent for MeODz, however, the vapor pressure is too high so that ACN solvent dries too quick. The vapor pressure of DMSO and 1-butanol are low, but MeODz has low solubilities in these solvents. So, the mixed solvents were used here. Then, the stamp with solvent ink on its surface was gently placed up-side down on the surface of SWCNT films and irradiated by Fiber-Lite MI-LED A2 high intensity LED illuminator (Dolan-Jenner industries Inc.). The relative air humidity was 3% and the room temperature was 22 °C.

2.3. Characterization of morphology and spectral properties

Atomic force microscropy (AFM) images were obtained in tapping mode by Cypher ES AFM (Asylum Research Corporation, CA). Scanning electron microscopy (SEM) image were taken on XEIA3 TESCAN SEM at an acceleration voltage of 10 kV. Broadband luminescent pattern images and luminescence spectra were captured by custom-built hyperspectral imaging system using previous methods.[16] In short, 730 nm laser was used as the excitation source. PL spectra were scanned from 950 to 1300 nm with an interval of 10 nm. Rhodamine B was dissolved in ACN/DMSO (v:v = 1:3) and ACN/1-butanol (v:v = 1:3) at 1 mg/mL, respectively. Then it was coated on PDMS stamp and patterned on SWCNT films using the same method without light irradiation. Zeiss LSM710 Confocal microscope was used to take the optical microscope images with an excitation laser of 405 nm.

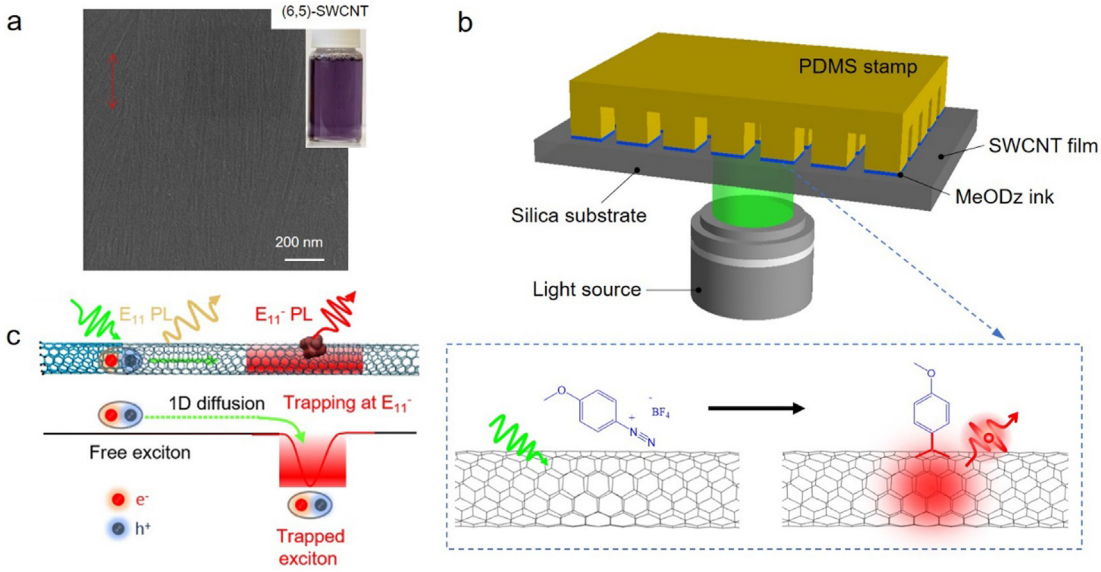

Fig. 1. a) SEM image of a thin film of aligned (6,5)-SWCNTs. The inset is a photograph of the purified (6,5)-SWCNT solution from which the thin film was made. b) Schematic representation of photo-patterning with 4-methoxybenzenediazonium tetrafluoroborate (MeODz) ink. The bottom shows light activated functionalization of a SWCNT by MeODz. c) The emission of E_{11} exciton from the pristine SWCNT and trapped E_{11}^- exciton from MeODz induced quantum defects.

3. Results and discussion

Highly purified (6,5)-SWCNTs films of a few layers (~6–7 nm thick) were aligned by vacuum filtration [14] for the photo-patterning (Fig. 1a, SI S1-S2, and the Experimental section). As illustrated in Fig. 1b, MeODz ink was coated on a Polydimethylsiloxane (PDMS) stamp, which was then brought into contact with the SWCNT film, and then irradiated by white light LEDs with a wavelength range of 400–750 nm (Fig. S3). The PDMS stamp used here features pillars with a radius of 2.5 μm at a pitch of 5 μm (SI S4). The stimulated visible light in resonance with (6,5)-SWCNTs can drive the photochemical reaction of diazonium with SWCNTs to covalently bond an aryl group to the SWCNTs forming the OCC quantum defect (inset of Fig. 1b) [17,18]. Besides photoluminescence (PL) from the mobile E_{11} excitons of the (6,5)-nanotube host, the photochemically created defects generate red-shifted $E_{\bar{1}1}$ PL from excitons trapped at the OCCs (Fig. 1c), which is used as a spectral signature to enable the resolution of the OCC-patterns on the thin-films [19].

To verify the feasibility of our proposed photo-patterning method, broadband hyperspectral PL images at 900–1550 nm wavelength range for the patterns prepared using different inks are compared as shown in Fig. 2. In the following, mixed solvents (ACN/DMSO or ACN/1-butanol at a volume ratio of 1:3) were used. For PDMS stamp coated by ACN/DMSO solvents without MeODz, there is only emission from E_{11} peak without luminescent patterns formed (Fig. 2a-b). By contrast, luminescent patterns are realized on ACN/DMSO solvents with 0.2 mg/mL MeODz (Fig. 2c). PL spectra show that the emission intensity of the white region corresponding to the PDMS pillars are higher than that of the black region between pillars (Fig. 2d). In comparison, for MeODz ink of ACN/1-butanol solvents (Fig. 2e), the luminescent patterns are opposite to that of ACN/DMSO solvents, where the emission intensity of the black region corresponding to the PDMS pillars are lower than that of the white region between pillars. In addition, although the loading force of PDMS stamp on the films is the same, the radius of the circle patterns in Fig. 2e is smaller than the radius of PDMS stamp pillar (2.5 μm), while that for MeODz ACN/DMSO ink in Fig. 2c is larger than 2.5 μm. Therefore, by changing the solvents used, the patterns can be tuned. Besides the original E_{11} peak at shorter wavelength from free excitons, both the white and black regions in Fig. 2c and e display $E_{\bar{1}1}$ (~1160 nm) peak, indicating the functionalization of both the regions with/without PDMS pillars (Fig. 2d and f). The lower emission intensity of both E_{11} and $E_{\bar{1}1}$ peaks for the black regions compared with that of the white regions may be due to the over-functionalization by more MeODz

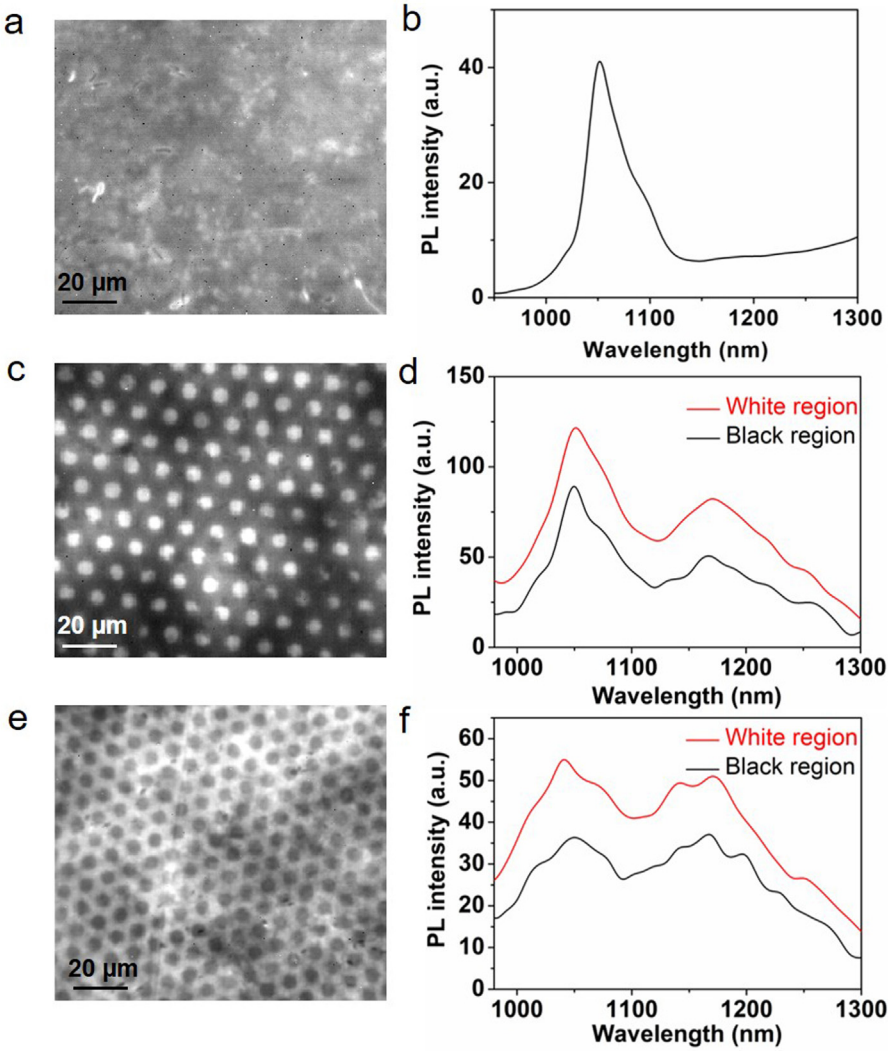

Fig. 2. Broadband PL images and spectra of the sample with PDMS stamp coated by ACN/DMSO solvents without MeODz (a-b), and with 0.2 mg/mL MeODz (c-d); and the sample with PDMS pattern coated by ACN/1-butanol solvents with 0.25 mg/mL MeODz (e-f).

Table 1
Comparison of different methods of photon-patterning with PDMS stamp.

Coating methods	Volume of ink used	Patterning methods	Patterns
Drop solution on PDMS stamp by pipette pillar	2 μL/cm^2	Dry the ink, then do the patterning;	No patterns found
	2 μL/cm^2	Do the patterning immediately after coating;	No patterns found
Use cotton swab to coat PDMS stamp	Tiny amount just to wet the surface of stamp	Do the patterning immediately after coating the ink	Patterns found

salts at the black region [20]. The details will be discussed later in the following part. To avoid the influence from the scattered light or probable luminescence from remnant MeODz on top of the films, all the films after photo-patterning were washed with deionized water before the measurements. Moreover, the bandpass image for the PL patterns at 1050 and 1150 nm with a bandwidth of 10 nm were also compared, both of which show the same patterns to that of the broadband PL patterns (SI S5).

It should be noted that the coating of PDMS stamp, the volume of ink used, the patterning methods, the solvents used, the concentration of MeODz and the patterning time all appear crucial for the generation and final styles of PL patterns. The optimal method is using a tiny amount of ink (<2 μL/cm^2) to just wet the surface of the PDMS stamp and do the patterning immediately after coating (Table. 1).

The surface of PDMS and SWCNT films are both hydrophobic. Thus, the ink with solvent of high polarity will have low wettability to react with SWCNT films. For example, water can dissolve MeODz very well; however, there is no patterns when using water as solvent (SI S6). For low concentration of ink, the contrast of the pattern is blurry (Fig. 3a for 0.1 mg/mL MeODz ACN/DMSO ink) or no patterns at all (Fig. 3c, 0.1 mg/mL MeODz ACN/1-butanol ink). While the contrast for the patterns using 1 mg/mL MeODz in both ACN/DMSO and ACN/1-butanol solvents are very obvious (Fig. 3b, and d). In addition, the increase of the patterning time from 6 min to 30 min leads to a more obvious pattern (Fig. 3e). To directly reveal the ink patterns, the PDMS stamp was coated with 1 mg/mL of Rhodamine B dissolved in ACN/DMSO and ACN/1-butanol solvents, instead of MeODz, as shown in the confocal microscope images of the patterns in Fig. 3f and g, respectively. For the Rhodamine B ink with ACN/DMSO solvents, the radius of the patterns is larger than the pillar radius of PDMS stamp of 2.5 μm (Fig. 3f). While that of the ACN/1-butanol solvent shows a smaller radius than 2.5 μm (Fig. 3g).

Based on the systematic investigation and comparison of the relative polarity and vapor pressure of the solvents used (Table. 2), the formation mechanism of photon-patterns can be understood as shown in Fig. 4. As the relative polarity of DMSO is smaller than 1-butanol, and the surface of PDMS and SWCNT thin-films are both hydrophobic, the ink that contains DMSO will have a relatively larger wettability and their contact angle on PDMS and SWCNT films will be smaller than that containing 1-butanol. The MeODz ACN/DMSO ink will not only coat the surface of PDMS pillars but also fills the gap between pillars (Fig. 4a), which is verified by in-situ hyperspectral broadband PL imaging (SI S7). While no or little ink can be found at the gap between PDMS pillars for that containing 1-butanol (Fig. 4b). As the vapor pressure of DMSO is much smaller than that of 1-butanol, there is still ink at the gap between PDMS pillars a few minutes later after the contact, while only little ink can be found on PDMS pillars (Fig. 4a). With the evaporation of the ink, it will form a circle with radius larger than that of PDMS pillars due to the existence of more solvents at the gap between pillars. For the ink containing 1-butanol, the relatively larger contact angle and the higher vapor pressure will lead to the accumulation of inks all around PDMS pillars with the faster evaporation of ink at the gap between PDMS pillars. As time goes

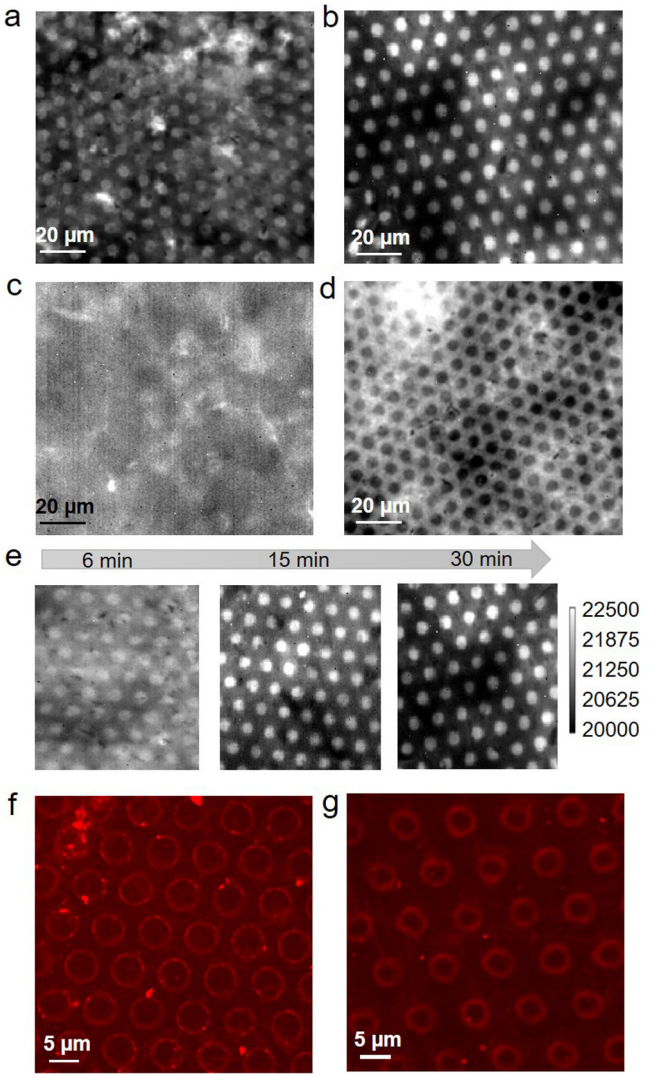

Fig. 3. Broadband PL images of 0.1 (a, c) and 1 (b, d) mg/mL MeODz coated PDMS patterns with MeODz dissolved in ACN/DMSO (a, b) and ACN/1-butanol (c, d) solvents. (e) Broadband PL images of patterns generated with 1 mg/mL MeODz in ACN/DMSO (1:3) irradiated by white light for different time. The broadband PL images are at the wavelength range of 900–1550 nm. Confocal microscope images of PDMS patterns with 1 mg/mL Rhodamine B in ACN/DMSO (f) and ACN/1-butanol solvents (g).

Table 2
Vapor pressure and relative polarity of solvents used.

Solvent	Vapor pressure (20°c, hpa)	Relative polarity
Water	17.5	1.000
Acetonitrile (ACN)	97	0.460
1-butanol	6.3	0.586
dimethylsulfoxide (DMSO)	0.61	0.444

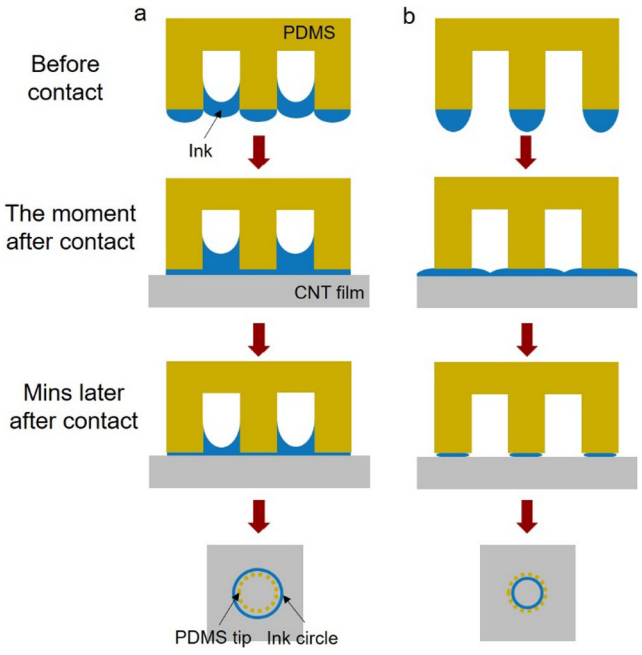

Fig. 4. Distribution of MeODz ink on PDMS patterned pillars and SWCNT films before and after contact. a, MeODz in ACN/DMSO solvents; b, MeODz in ACN/1-butanol solvents.

on, only ink on PDMS pillars is there, leading to a smaller circle is smaller than that of PDMS pillars (Fig. 4b). This hypothesis is also consistent with the patterns in Fig. 2c and e, where the functionalization extent of SWCNT films at the regions with less ink left will have a brighter image than that at the regions with more ink left.

4. Conclusion

In summary, we present a facile, low cost and scalable method to photo-patterning organic color centers on (6,5)-SWCNT films with high spatial accuracy. Light-driven diazonium chemistry is used to functionalize SWCNT with MeODz ink coated on PDMS stamp by micro-contact printing. Emission at 1050 nm from E_{11} peak of pristine SWCNT and 1150 nm from E_{11}^{-} peak of functionalized SWCNT can be observed at both sites patterned with PDMS pillars or the gap between pillars. The polarity and vapor pressure of the solvents, the volume of ink used, the patterning methods, the concentration of MeODz, and the patterning time all appear crucial for the patterning. By carefully design these parameters, the size and morphology of the luminescent patterns can be modulated accordingly. It is promising that the patterning at molecular level with high spatial resolution and chemical precision can be obtained by optimizing the solvent chemistry and the printing methods, such as using nano-printing methods (dip-pen nanolithography [21], scanning probe lithography [22]). This method could also promote the development and applications of patterning technology for other solid-state films, such as 2D transition metal dichalcogenides [23], at molecular level for quantum techniques and other chip-integrated nanoelectronics and optoelectronic applications.

Declaration of Competing Interest

The authors declare that they have no known competing financial interests or personal relationships that could have appeared to influence the work reported in this paper.

Acknowledgments

B. X. acknowledges the support from the National Natural Science Foundation of China (Grant No. 62005240), Fundamental Research Funds for the Central Universities, the Open Fund of the State Key Laboratory of Modern Optical Instrumentation of Zhejiang University, and Zhejiang University K.P.Chao's High Technology Development Foundation. Y.H.W. gratefully acknowledges the support from the National Science Foundation through award number PHY1839165. The work also makes use of instrumentation components funded in part by NSF (CHE-1904488) and NIH/NIGMS (Grant No. R01GM114167).

Appendix A. Supplementary material

Supplementary data to this article can be found online at https://doi.org/10.1016/j.matdes.2021.110252.

References

[1] A.H. Brozena, M. Kim, L.R. Powell, YuHuang Wang, Controlling the optical properties of carbon nanotubes with organic colour-centre quantum defects, Nat. Rev. Chem. 3 (6) (2019) 375–392.
[2] X. He, H. Htoon, S.K. Doorn, W.H.P. Pernice, F. Pyatkov, R. Krupke, A. Jeantet, Y. Chassagneux, C. Voisin, Carbon nanotubes as emerging quantum-light sources, Nat. Mater. 17 (8) (2018) 663–670.
[3] M. Nutz, J. Zhang, M. Kim, H. Kwon, X. Wu, YuHuang Wang, A. Högele, Photon Correlation Spectroscopy of Luminescent Quantum Defects in Carbon Nanotubes, Nano Lett. 19 (10) (2019) 7078–7084.
[4] H. Kwon, M. Kim, B. Meany, Y. Piao, L.R. Powell, YuHuang Wang, Optical Probing of Local pH and Temperature in Complex Fluids with Covalently Functionalized, Semiconducting Carbon Nanotubes, J. Phys. Chem. C 119 (7) (2015) 3733–3739.
[5] A.L. Ng, C.-F. Chen, H. Kwon, Z. Peng, C.S. Lee, YuHuang Wang, Chemical Gating of a Synthetic Tube-in-a-Tube Semiconductor, J. Am. Chem. Soc. 139 (8) (2017) 3045–3051.
[6] A.K. Mandal, X. Wu, J.S. Ferreira, M. Kim, L.R. Powell, H. Kwon, L. Groc, Y. Wang, L. Cognet, Fluorescent sp(3) Defect-Tailored Carbon Nanotubes Enable NIR-II Single Particle Imaging in Live Brain Slices at Ultra-Low Excitation Doses, Sci. Rep. 10 (1) (2020) 5286.
[7] X. He, N.F. Hartmann, X. Ma, Y. Kim, R. Ihly, J.L. Blackburn, W. Gao, J. Kono, Y. Yomogida, A. Hirano, T. Tanaka, H. Kataura, H. Htoon, S.K. Doorn, Tunable room-temperature single-photon emission at telecom wavelengths from sp3 defects in carbon nanotubes, Nat. Photon. 11 (9) (2017) 577–582.
[8] Y.-C. Chen, P.S. Salter, M. Niethammer, M. Widmann, F. Kaiser, R. Nagy, N. Morioka, C. Babin, J. Erlekampf, P. Berwian, M.J. Booth, J. Wrachtrup, Laser Writing of Scalable Single Color Centers in Silicon Carbide, Nano Lett. 19 (4) (2019) 2377–2383.
[9] J. Wang, Y. Zhou, X. Zhang, F. Liu, Y. Li, K. Li, Z. Liu, G. Wang, W. Gao, Efficient Generation of an Array of Single Silicon-Vacancy Defects in Silicon Carbide, Phys. Rev. Appl. 7 (6) (2017) 064021.
[10] W. Zheng, T. Xie, Y. Zhou, Y.L. Chen, W. Jiang, S. Zhao, J. Wu, Y. Jing, Y. Wu, G. Chen, Y. Guo, J. Yin, S. Huang, H.Q. Xu, Z. Liu, H. Peng, Patterning two-dimensional chalcogenide crystals of Bi_2Se_3 and In_2Se_3 and efficient photodetectors, Nat. Commun. 6 (1) (2015) 6972.
[11] B.J. Ravoo, Microcontact chemistry: surface reactions in nanoscale confinement, J. Mater. Chem. 19 (47) (2009) 8902–8906.
[12] C. Hamon, M. Henriksen-Lacey, A. La Porta, M. Rosique, J. Langer, L. Scarabelli, A.B.S. Montes, G. González-Rubio, M.M. de Pancorbo, L.M. Liz-Marzán, L. Basabe-Desmonts, Tunable Nanoparticle and Cell Assembly Using Combined Self-Powered Microfluidics and Microcontact Printing, Adv. Funct. Mater. 26 (44) (2016) 8053–8061.
[13] H. Kwon, A. Furmanchuk, M. Kim, B. Meany, Y. Guo, G.C. Schatz, YuHuang Wang, Molecularly Tunable Fluorescent Quantum Defects, J. Am. Chem. Soc. 138 (21) (2016) 6878–6885.
[14] X. He, W. Gao, L. Xie, B.o. Li, Q.i. Zhang, S. Lei, J.M. Robinson, E.H. Hároz, S.K. Doorn, W. Wang, R. Vajtai, P.M. Ajayan, W.W. Adams, R.H. Hauge, J. Kono, Wafer-scale monodomain films of spontaneously aligned single-walled carbon nanotubes, Nat. Nano. 11 (7) (2016) 633–638.
[15] J. Huang, A.L. Ng, Y. Piao, C.-F. Chen, A.A. Green, C.-F. Sun, M.C. Hersam, C.S. Lee, YuHuang Wang, Covalently Functionalized Double-Walled Carbon Nanotubes Combine High Sensitivity and Selectivity in the Electrical Detection of Small Molecules, J. Am. Chem. Soc. 135 (6) (2013) 2306–2312.
[16] B. Xu, X. Wu, M. Kim, P. Wang, YuHuang Wang, Electroluminescence from 4-nitroaryl organic color centers in semiconducting single-wall carbon nanotubes, J. Appl. Phys. 129 (4) (2021) 044305, https://doi.org/10.1063/5.0039047.
[17] L.R. Powell, Y. Piao, YuHuang Wang, Optical Excitation of Carbon Nanotubes Drives Localized Diazonium Reactions, J. Phys. Chem. Lett. 7 (18) (2016) 3690–3694.

[18] X. Wu, M. Kim, H. Kwon, YuHuang Wang, Photochemical Creation of Fluorescent Quantum Defects in Semiconducting Carbon Nanotube Hosts, Angew. Chem. In. Ed. 57 (3) (2018) 648–653.
[19] Z. Huang, L.R. Powell, X. Wu, M. Kim, H. Qu, P. Wang, J.L. Fortner, B. Xu, A.L. Ng, YuHuang Wang, Photolithographic Patterning of Organic Color-Centers, Adv. Mater. 32 (14) (2020) 1906517, https://doi.org/10.1002/adma.v32.1410.1002/adma.201906517.
[20] Y. Piao, B. Meany, L.R. Powell, N. Valley, H. Kwon, G.C. Schatz, YuHuang Wang, Brightening of carbon nanotube photoluminescence through the incorporation of sp3 defects, Nat. Chem. 5 (10) (2013) 840–845.
[21] P.-C. Chen, X. Liu, J.L. Hedrick, Z. Xie, S. Wang, Q.-Y. Lin, M.C. Hersam, V.P. Dravid, C.A. Mirkin, Polyelemental nanoparticle libraries, Science 352 (6293) (2016) 1565–1569.
[22] Z. Huang, L.e. Li, X.A. Zhang, N. Alsharif, X. Wu, Z. Peng, X. Cheng, P. Wang, K.A. Brown, YuHuang Wang, Photoactuated Pens for Molecular Printing, Adv. Mater. 30 (8) (2018) 1705303, https://doi.org/10.1002/adma.v30.810.1002/adma.201705303.
[23] D. Voiry, A. Goswami, R. Kappera, C.d.C.C.e. Silva, D. Kaplan, T. Fujita, M. Chen, T. Asefa, M. Chhowalla, Covalent functionalization of monolayered transition metal dichalcogenides by phase engineering, Nat. Chem. 7 (1) (2015) 45–49.